

AD-A034 116

TEXAS INSTRUMENTS INC DALLAS EQUIPMENT GROUP
VIDEO CONTROLLED FLIR FOCUS.(U)

F/G 17/5

NOV 76 E ELWELL, J LEWIS, K STELZENMULLER

F33615-75-C-1197

AFAL-TR-76-161

NL

UNCLASSIFIED

1 OF 1
AD-A
034 116



END
DATE
FILMED
2-25-77
NTIS

U.S. DEPARTMENT OF COMMERCE
National Technical Information Service

AD-A034 116

VIDEO CONTROLLED FLIR FOCUS

TEXAS INSTRUMENTS, INC.
DALLAS, TEXAS

NOVEMBER 1976

ADA034116

011173

AFAL-TR-76-161

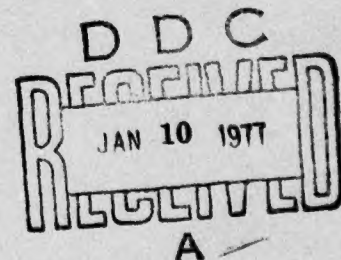
VIDEO CONTROLLED FLIR FOCUS

*EQUIPMENT GROUP
ELECTRO-OPTICS DIVISION
TEXAS INSTRUMENTS INCORPORATED
DALLAS, TEXAS 75222*

NOVEMBER 1976

TECHNICAL REPORT AFAL-TR-76-161
FINAL REPORT FOR PERIOD JUNE 1975 - MAY 1976

Approved for public release; distribution unlimited



AIR FORCE AVIONICS LABORATORY
AIR FORCE WRIGHT AERONAUTICAL LABORATORIES
AIR FORCE SYSTEMS COMMAND
WRIGHT-PATTERSON AIR FORCE BASE, OHIO 45433

REPRODUCED BY
NATIONAL TECHNICAL
INFORMATION SERVICE
U.S. DEPARTMENT OF COMMERCE
SPRINGFIELD, VA. 22161

NOTICE

When Government drawings, specifications, or other data are used for any purpose other than in connection with a definitely related Government procurement operation, the United States Government thereby incurs no responsibility nor any obligation whatsoever; and the fact that the government may have formulated, furnished, or in any way supplied the said drawings, specifications, or other data, is not to be regarded by implication or otherwise as in any manner licensing the holder or any other person or corporation, or conveying any rights or permission to manufacture, use, or sell any patented invention that may in any way be related thereto.

This report has been reviewed by the Information Office (IO) and is releasable to the National Technical Information Service (NTIS). At NTIS, it will be available to the general public, including foreign nations.

This technical report has been reviewed and is approved for publication.

Edward J. Susedik

EDWARD J. SUSEDIK
Project Engineer, FLIR Group
FOR THE COMMANDER

Gerald J. Shroyer

GERALD J. SHROYER
Acting Chief, FLIR Group

Harold E. Geltmacher

HAROLD E. GELTMACHER, ACTG CHIEF
Electro-Optics & Reconnaissance Branch
Reconnaissance & Weapon Delivery Division

ASSESSMENT	
NTIS	✓
SEC	
UNCLASSIFIED	
RESTRICTED	
BY	
DISTRIBUTION AVAILABLE	
DATE	
A	

Copies of this report should not be returned unless return is required by security considerations, contractual obligations, or notice on a specific document.

UNCLASSIFIED

SECURITY CLASSIFICATION OF THIS PAGE (When Data Entered)

REPORT DOCUMENTATION PAGE		READ INSTRUCTIONS BEFORE COMPLETING FORM
1. REPORT NUMBER AFAL-TR-76-161	2. GOVT ACCESSION NO.	3. RECIPIENT'S CATALOG NUMBER
4. TITLE (and Subtitle) Final Technical Report For Video Controlled FLIR Focus		5. TYPE OF REPORT & PERIOD COVERED Final Technical Report June 5, 1975 - May 31, 1976
7. AUTHOR(s) E. Elwell J. Lewis K. Stelzenmuller		6. PERFORMING ORG. REPORT NUMBER
9. PERFORMING ORGANIZATION NAME AND ADDRESS Texas Instruments Inc. Equipment Group P.O. Box 6015 Electro-Optics Div. 13500 N. Central Expressway, Dallas, Texas 75222		8. CONTRACT OR GRANT NUMBER(s) AF33615-75-C-1197
11. CONTROLLING OFFICE NAME AND ADDRESS Air Force Avionics Laboratory Air Force Systems Command Wright-Patterson AFB, Ohio 45433		10. PROGRAM ELEMENT, PROJECT, TASK AREA & WORK UNIT NUMBERS 20040602
14. MONITORING AGENCY NAME & ADDRESS (if different from Controlling Office)		12. REPORT DATE November 1976
		13. NUMBER OF PAGES 31
		15. SECURITY CLASS. (of this report) UNCLASSIFIED
		15a. DECLASSIFICATION/DOWNGRADING SCHEDULE
16. DISTRIBUTION STATEMENT (of this Report) Approved for Public Release, Distribution Unlimited		
17. DISTRIBUTION STATEMENT (of the abstract entered in Block 20, if different from Report)		
18. SUPPLEMENTARY NOTES		
19. KEY WORDS (Continue on reverse side if necessary and identify by block number) FLIR - Forward Looking Infrared		
20. ABSTRACT (Continue on reverse side if necessary and identify by block number) This report covers the effort under Air Force contract number F33615-75-C-1197 for the Video Controlled FLIR Focus. The stated objective of this program was to invent, design, breadboard and demonstrate an automatic focusing device and a dynamic range expansion system to be used with FLIR sensors. The scene analysis, breadboard implementation and test results of both tasks are covered in this report.		

DD FORM 1 JAN 73 1473 EDITION OF 1 NOV 65 IS OBSOLETE

UNCLASSIFIED

SECURITY CLASSIFICATION OF THIS PAGE (When Data Entered)

FOREWORD

This research was sponsored by the Air Force Avionics Laboratory under Project Number 2004, Task 06 and was performed by Texas Instruments Incorporated, 13500 North Central Expressway, Dallas, Texas 75222. The contract number was F33615-75-C-1197. The principal investigator was Mr. Joseph Lewis. The Air Force program monitor was Edward J. Susedik (AFAL/RWI). The research period was from June 1975 to May 1976.

TABLE OF CONTENTS

Paragraph	Title	Page
	SECTION I	1
1	Introduction - Video Control Focus Task	1
2	Scene Spectral Analysis	1
3	Design Breadboard System	4
4	System Test	6
5	Conclusions	7
	SECTION II	9
1	Introduction - DRE Task	9
2	DRE Circuit Description	9
3	Cumulative Distribution Technique	11
4	Comb Filter	15
5	Test Results	19
	LIST OF ILLUSTRATIONS	
1	Scene Description	2
2	Power Spectral Density Plot	3
3	Block Diagram Video Controlled FLIR Focus	5
4	Direct Method P(V) Block Diagram	10
5	Typical Waveforms Dynamic Range Enhancement Scheme 1	12
6	Dynamic Range Enhancement Scheme 2, Block Diagram	13
7	Coordinate Translation	16
8	DRE 1	17
9	DRE 2, 3, 4, 5	18
10	DRE Data Photos	22

FINAL TECHNICAL REPORT FOR THE
VIDEO CONTROLLED FLIR FOCUS PROGRAM

SECTION I

1. Introduction - Video Controlled Focus Task

Complex optical systems require that lens positions be varied to maintain optimum focus. This will maintain best focus with target range variations, temperature variations in the system and manufacturing tolerances of optical parts. In the past, this function has been left to the system operator, resulting in distraction from scene interpretation. In addition, for infrared systems, athermalization of the optical elements requires greater mechanical correction than for systems using visible wavelengths due to the lens material characteristics.

The objective of this task was to use video signals from a parallel scan Forward Looking Infrared (FLIR) system to sense the loss of optimum focus and apply a correcting signal to a lens positioning system. The first stage of investigation consisted of analyzing the spectral content of the summed signal from the FLIR preamplifiers as a function of degree of focus. From this data, a suitable band of frequencies was chosen such that the high frequency energy in the video signal changed sharply with changes in focus. Next, a breadboard system was constructed to analyze changes in this high frequency energy and to make a decision to move the focus lens in one direction or the other. Finally tests of the breadboard circuit were performed both on a collimator and using real world targets with a FLIR system.

2. Scene Spectral Analysis

Preliminary work on the Video Controlled FLIR Focus involved taking spectra of various FLIR scenes to determine how the spectral distribution changed with focus changes. Figure 1 is a partial list of representative scenes that were used in the analysis. The spectra for scene 5 is shown in Figure 2 and is typical of the scenes analyzed. Tests were made for all scenes combining 5, 10 or 20 channels at a time, with the sum of 20 channels showing slightly more variation in high frequency energy for different degrees of focus. The different spectra in Figure 2 have been individually normalized, which precludes direct comparison of signal amplitudes, however; changes in the relative sizes of high and low frequency regions can be seen. Slightly out of focus represents about 50% reduction in MTF at twice the normal system resolution. Grossly out of focus represents the manual control at its extreme rear limit, approximately 500 feet. The general shape of the various curves is the familiar $1/f$ distribution, however; certain scenes show pronounced peaks and low regions so that little generalization is possible. It was generally assumed that the high frequency energy would decrease more for a given amount of defocus than mid frequencies, but several examples showed that this was not universal. This leads to the conclusion that a fairly wide band of frequencies should be monitored to gain a more general sensitivity function.

SCENE NUMBER

SCENE DESCRIPTION

- | | |
|---|---|
| 1 | UNDERPASS 3900 FEET |
| 2 | ANTENNA AND SOUTH BLD
2400 FEET |
| 3 | DOWNTOWN DALLAS FAR FIELD
ORANGE TANKS EAST OF BLD
3900 FEET AWAY |
| 4 | CYCLONE FENCE IN PARKING LOT
800 FEET |
| 5 | TREES AND BLDs 1100 FEET |
| 6 | PASTURE 4000 FEET
LIGHT POLE FOREGROUND |
| 7 | GAS EXHAUST
FLAME NEAR NCG
2000 FEET |

Figure 1.

POWER SPECTRAL DENSITY PLOT

SCENE 5

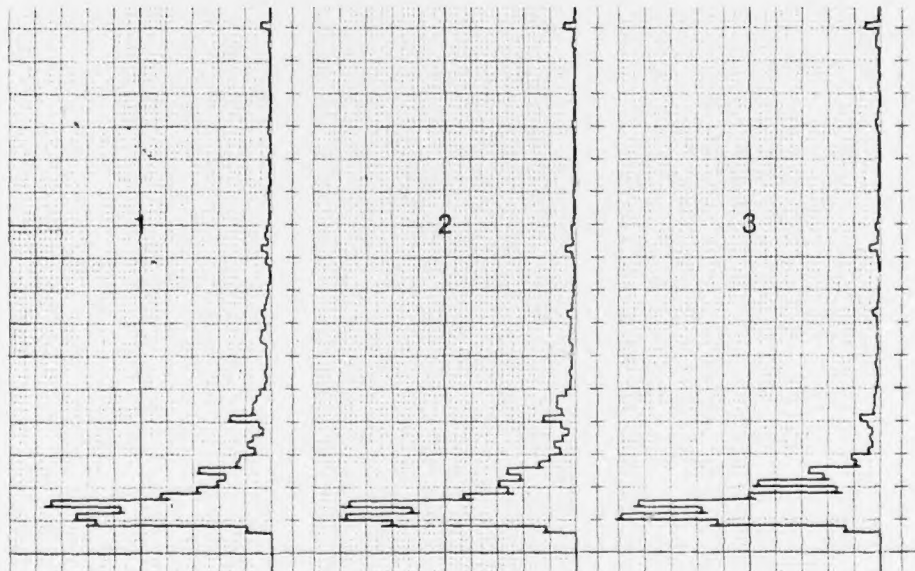
TREES AND BLDG
1100 FEET

BW 1KHz/DIV
 $\Delta f = 200\text{Hz}$
126 FREQ BINS .05cm ea
(1/2 MINOR DIVISION)

IN FOCUS

SLIGHTLY OUT
OF FOCUS

GROSSLY OUT
OF FOCUS



SUM OF 20 CHANNELS

Figure 2. Scene 5

The central forty channels of the system were chosen as the region of interest for the breadboard Video Controlled Focus System. Provision was made for optional inversion of the signals of each group of ten nonconsecutive channels. The inversion was conceived to have less sensitivity to the exact angular orientation of scenes, and to offer more immunity to various forms of common mode noise from motors and powerful switching waveforms in the television portion of the FLIR. Tests indicated that inversion produces almost the same change in the spectral energy as noninverted video but with definite reduction in the narrow band noise from the television system.

3. Design of Breadboard System

The basic result of the scene analysis was the selection of the video passband to be monitored at 3 KHz to 23 KHz, with the signals from 40 channels summed together. Figure 3 is a block diagram of the breadboard video controlled focus system. The operation is as follows:

Signals from 40 channels are sampled and added together in groups of 10 through 4 buffer amplifiers. These groups are then summed to form a single signal which is then filtered to produce the desired passband. To form a voltage proportional to the amount of AC signal present, a full wave rectifier processes the signal which is then filtered down to a frequency of 5 to 10 Hz. The resulting voltage is proportional to the amount of detail in the scene, the inherent contrast in the different objects in the scene and the amount of noise present, as well as the degree of focus. This voltage is sampled periodically with a sample and hold circuit and the sample from the previous period is held in a second identical circuit. These two signals are compared to determine if the new sample has a higher or lower level than the previous sample. The basic concept of the system is that a higher level indicates the scene is in better focus than before and a lower level, indicates a worse focus condition.

The lens position is stepped either forward or backward every period and the direction of movement is stored in a JK flip-flop. If focus is improving, the next command will be in the same direction as the previous one. If the focus is not improving, the flip-flop toggles and a step is made in the opposite direction. The comparator's digital signal is changed into a bi-directional analog pulse which is integrated to form a staircase waveform as the system output. The output voltage is used directly as the command signal to the existing FLIR focus servo system. The pulse generator produces the timing pulses for the various operations.

The first breadboard circuit used analog sample and hold circuits and an analog comparator. The preliminary tests indicated that there were problems of leakage and gain balance between these analog stages. Therefore, the decision was made to use an analog to digital converter and digital latches and comparator. Using the digital approach not only nullifies drift problems but allows later interfacing with a digital implementation of the pulse forming and integration stages.

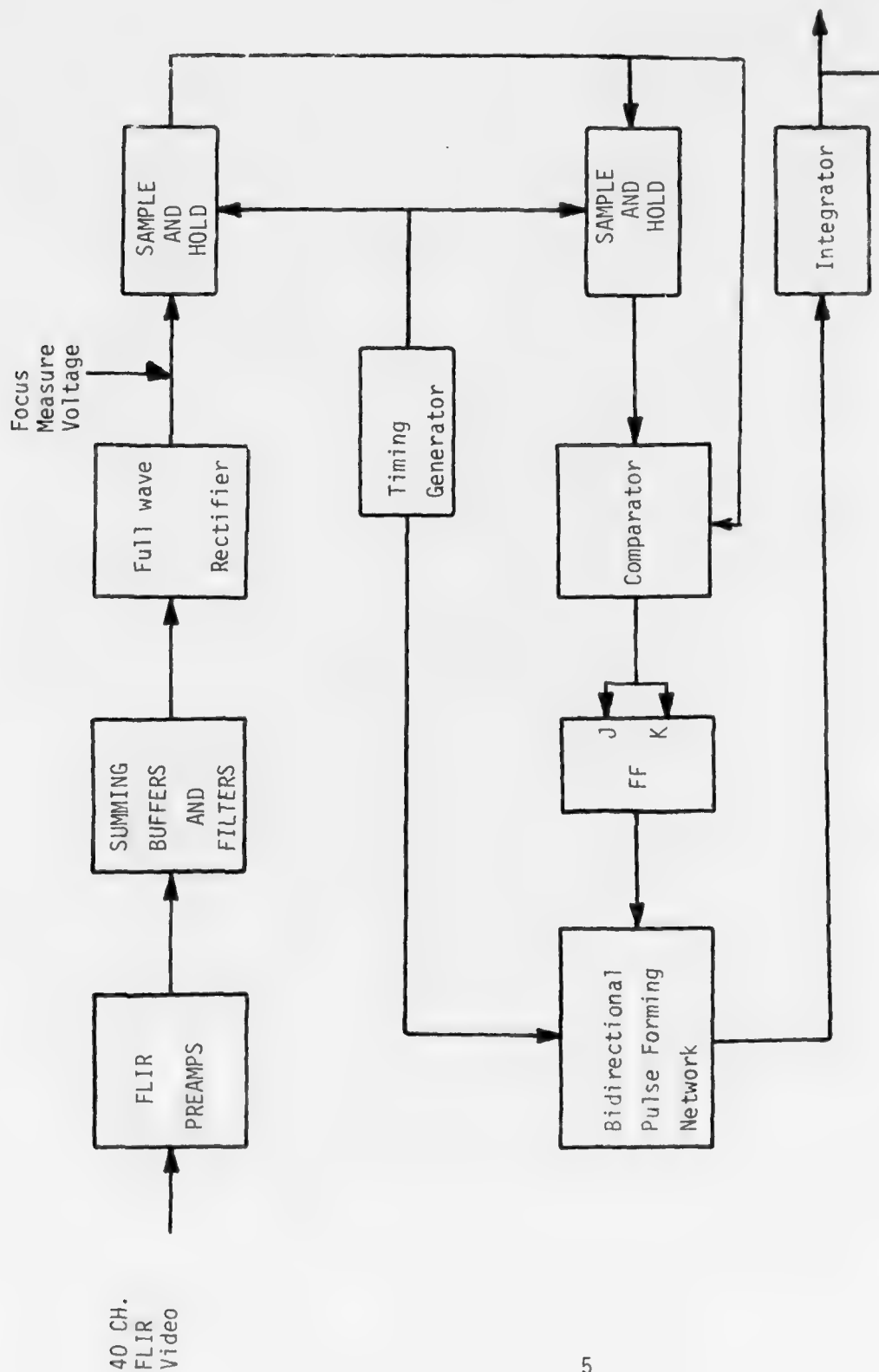


Figure 3. Block Diagram Video Controlled FLIR Focus

Due to their secondary nature, there were two areas not addressed during this investigation which should be considered. The first consideration being to provide video controlled focus for wide field of view (WFOV). The depth of focus in WFOV is large and a useable image is obtained over most of the range of adjustment, therefore; video controlled focus may not be necessary. If implementing the video focus in this field of view proves necessary, it should be accomplishable by readjusting the focus step size. The second item is to provide a search procedure when starting from such a degree of defocus such that no improvement or impairment can be detected with lens movements. The action of the breadboard is to oscillate one step about the last position until an increase in focus measure voltage is encountered but no far ranging search is started. Such a feature would be relatively straight forward to implement but its action would be independent of the main circuitry.

4. Systems Tests

The first tests on the system involved checking the FLIR system's focus servo system for speed of operation. The measurements were made at the lens position sensing potentiometer where the voltage varies linearly with focus lens position. The range of travel available to the video controlled focus was from about 500 feet to infinity. The voltages measured on the FLIR focus servo PWB were -1.2 volts at 500 feet and +1.2 volts at infinity. The slew rate was measured at 1 volt per second. This corresponds to a closing rate of about 120 kts at a 500 foot range. The closing rate capability is proportional to the square of the instantaneous target range, so that at most ranges this servo system can slew fast enough to handle expected closing rates. The bandwidth of the servo system is between 2 and 3 Hz which is adequate to handle the 1 sample per second step rates used in system tests but inadequate to handle a more desirable rate of 10 samples per second. The last factor investigated in the servo system was the repeatability of lens position for given command signals. The factors which affect this parameter are electrical loop gain, mechanical stiction and play in the gear train. The average lens position error in a series of repeatability runs was about 6.6% of the lens travel between 500 feet and infinity. This value is fairly large, representing about 50% reduction in MTF for a nominal resolution target.

Tests were then performed with the breadboard video controlled focus system, to determine the sensitivity of focus variation. Standard four-bar targets were viewed from a collimator and the change in focus measure voltage was recorded using temperature differences of 30°C. The best focus was determined visually and the worst case was taken as either extreme of the focusable lens travel. The following chart illustrates the magnitude of variations:

Relative Target Size

Best to Worst Voltage Change

0.143	8 mV
0.2	11 mV
0.417	730 mV
0.75	2200 mV

The residual focus measure voltage present with the lens covered was fairly consistently measured to be about 80 mV. There was, however, a random variation in this signal which appears to have a $1/f$ distribution with an amplitude of 3 to 10 mV peak. As can be seen, this could be a very significant fraction of the best to worst focus dependent voltage change and could cause erratic operation of subsequent circuitry.

The third set of system test consisted of observing real world scenes. The magnitude of best to worst focus measure voltage was expected to be considerably higher for normal scenes than for single small targets due to the increased detail in the image. This was found to be true, with changes of 50 to 100mV being common. Very high contrast objects such as exhaust stacks naturally provided much higher variation but are not truly representative of most scenes. Here, investigation of the focus measure voltage showed a somewhat higher level of variation for real scenes often running 10 to 20 mV peak in an apparently random manner.

The previous efforts were obtained with the focus being varied manually. These final tests consisted of using the remainder of the video controlled focus circuitry to drive the FLIR focus. Both collimator and real world targets were used and the maximum deviations of the lens position from the optimum were observed. The results hinge around setting a certain minimum size of steps in the command signal which is approximately 0.25V measured at the focus command input. Steps of less than this value caused very erratic operation due to insufficient change in the focus measure voltage compared to the random noise. Above this value the system operates more or less as intended but occasional incorrect decisions are made by the circuitry. Another problem is that in order to obtain this relatively accurate operation, the scene must be defocused by an amount (step size) that is fairly noticeable. The test results indicated that on real world scenes at three different ranges on 0.4 mR targets or larger, the system never exceeded four steps in either direction and was usually confined to two or fewer steps about best focus. Nevertheless, the peak deviation is approximately equivalent to 50% modulation reductions for a 0.4 mR target and consequently larger reductions for smaller targets. The design goal parameters of the system calls for 5% reduction of MTF from optimum.

5. Conclusions

The tests to date of the video controlled FLIR focus indicate that this low focus step rate system does not provide sufficient focus-dependent-signal to noise to ensure proper operation on a variety of normally encountered scenes. The sources of the offending noise are $1/f$ modulated noise from the detectors themselves, small amounts of jitter and variations in the scene itself. Because of the extra sensitivity to high frequencies of the circuit these affects may be too subtle to be apparent directly to the eye.

There are alternative places to sense the video signals other than the output of the FLIR preamplifiers. This point was chosen to eliminate the gating pulses and the variable gain effects associated with the output of the postamplifiers. The postamplifiers do offer a much better signal level with which to work and an automatically (and slowly) varied gain might allow a system to work over a wider range of real world scenes since the available dynamic range is used to fullest advantage. Another possible point to monitor would be in the television video output. This would offer extreme ease of connection, substituting one wire for 40 or more. This however, translates the operating frequencies upward to a region that is considerably more difficult to design in the necessary functions. In addition, the MTF variation at this point is even less like the ideal lens defocusing variation and the signal to noise inevitably suffers some additional loss in traversing more electrical circuitry and optical elements.

An approach has been suggested by the Air Force Weapons Laboratory's video controlled focus system. There are too many differences between the systems, such as spectral region and scan method, to allow a direct comparison of results, but the high speed focus variations, 15 Hz, was described as of major importance. A similar method for modular FLIR systems might be developed by inserting high speed optical wedges into the optical path to modulate the system focus. By maintaining synchronism with the scanner and using synchronous demodulation techniques, the circuitry should be able to filter the command signal sufficiently to effectively eliminate response to noise induced errors. The FLIR lens system would need only to respond to temperature and range induced focus shifts and not to the modulation (step) rate. The basic improvement in going to a high speed design is due to the increase in the focus information in the presence of the same amount of noise. The filtering, rectifying and sampling circuitry would need improvement over the current level however, in order to gain the expected benefits. Finally, the video controlled focus can possibly be improved over the current level of effectiveness but there will remain the problems of ambiguities due to scenes with multiple targets at different ranges and scenes with very low contrast or detail that will cause occasional differences from optimum focus.

DYNAMIC RANGE ENHANCEMENT

SECTION II

1. Introduction

An AC coupled non-DC restored FLIR video chain is subject to video level shifts caused by large temperature differences in the field-of-view (FOV). It is desirable, in most cases, to view detail in both the high and low temperature areas simultaneously, thus; DC restoration is not the answer to the problem.

The purpose of the "Dynamic Range Enhancement" study was to investigate methods of compressing the video amplitude while maintaining high frequency response. It was also to develop a technique of restoring the compressed video to its proper grey shade level in the video amplitude spectrum.

FLIR targets, which cause level shifts in the mean value of the video, are of the step function type and vary widely in pulse width and amplitude. One method of reducing the step function amplitude is to remove several of the low frequency components of the target. When this is achieved, the dynamic range requirements of the following video stages are reduced and all detail in both temperature areas can be displayed together on the limited dynamic range of the video monitor. Most video monitors have a useful dynamic range in the area of 32 to 40 dBs and is necessary to center the video level in this useful range of display capability.

A method was developed by Texas Instruments which analyzes any video mean value shift due to AC coupling and then restores the compressed video to its proper DC level with respect to the rest of the scene. Two circuit implementations were investigated, both of which calculate the probability density ($P(V)$) function of video amplitude and extract the mean and mode values of $P(V)$ as correction signals for the following line of display video.

2. DRE Circuit Description

Figure 4 is a block diagram of a circuit which plots the $P(V)$ curve for each line of video during the horizontal blanking interval following the line. A function switch is included in the design to allow the circuit to either plot out the complete $P(V)$ curve or locate the peak of the $P(V)$ function and then hold the voltage coordinate at the maximum point. The circuit operation is as follows: The video input is compared to DC levels which represent 1/2 grey shade increments in the amplitude spectrum. When any comparator's video input is above its reference, the output is high. For any instantaneous level of video input, a group of comparator outputs will be high and a group whose outputs will be low. For example, if the video amplitude is between V_3 and V_4 , comparators #1 thru #3 will have high outputs and comparators #4 and #5 will have low outputs. As a result, there will be one exclusive OR gate whose output is high. The exclusive OR output is integrated over the entire line of video. The integrator input is "one" when the video is within its half grey shade limits and is a "zero" when

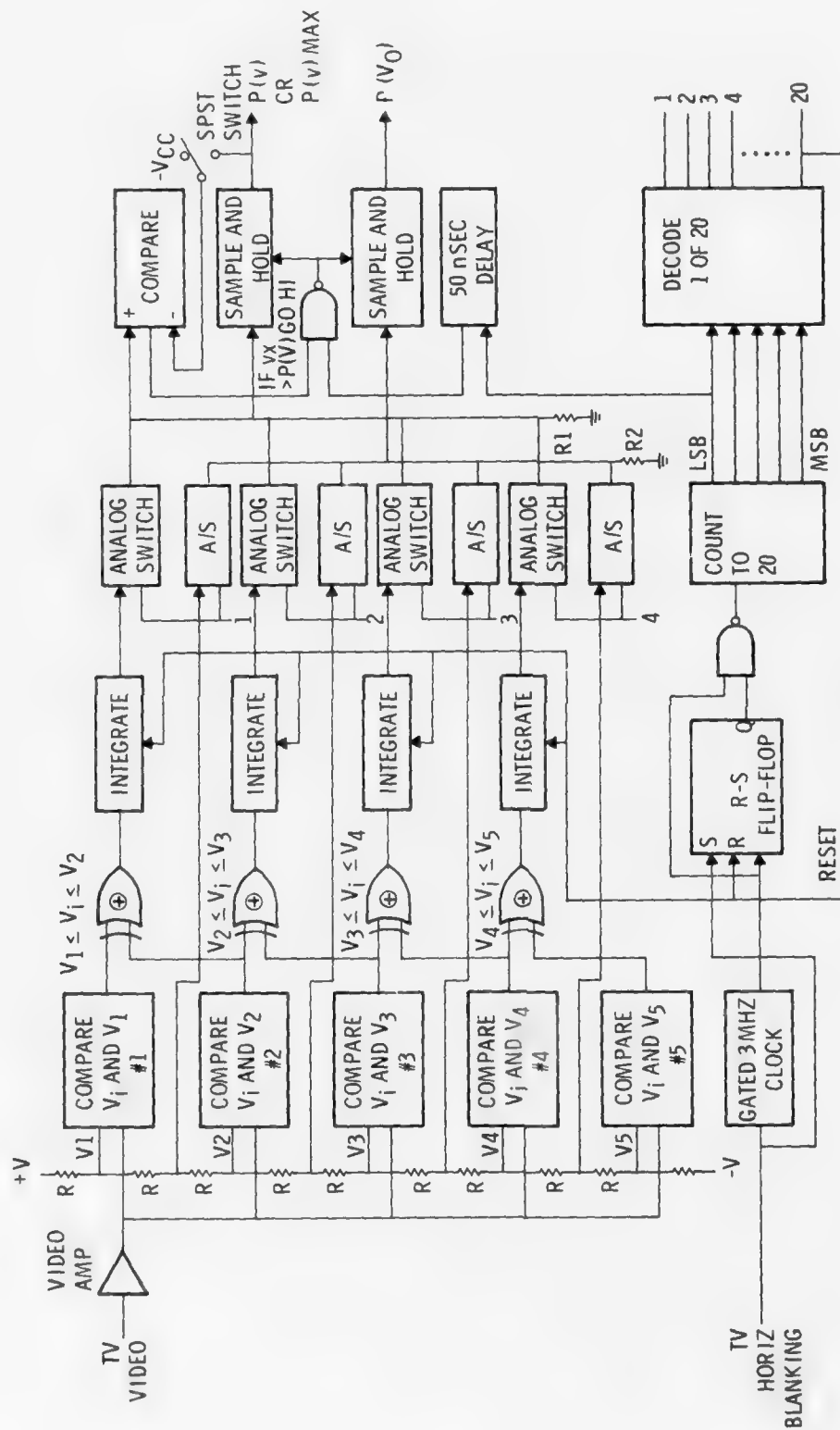


Figure 4. Direct Method $P(V)$ Block Diagram

the video is outside its limits. Therefore, the voltage value that an integrator reaches is linearly related to the total amount of video contained within its half grey shade limits. All of the integrator outputs are sampled sequentially by the controller during the horizontal blanking interval and a $P(V)$ curve is developed across $R1$. Waveforms are shown in Figure 5.

From the $P(V)$ curve developed across $R1$ it is necessary to locate the peak since the coordinate of the peak of $P(V)$ is that level where most of the video lies. When the video is AC coupled, its mean value is zero, thus; no correction level needs to be added to the line of video. If, however; the coordinate of the mode (peak of $P(V)$) is different than zero, a correction voltage equal to the coordinate of the mode should be added to the video. This will correct the background level which has been depressed by high variance targets. To locate the mode of $P(V)$ the voltage across $R1$ is compared to the voltage that was across $R1$ for the previous sample. The previous level is stored in the sample & hold. When the previous sample is greater, the $P(V)$ comparator output is low and the next value is compared against the sample & hold output. When a value across $R1$ is greater than the sample & hold value, the comparator output goes high and the new value is inserted in the sample & hold. Therefore; after all samples have been completed the highest value is located in the sample & hold.

A similar sample & hold is maintaining the value of the coordinate of the mode $P(V_0)$, and this value becomes the correction voltage if different than zero. The mode of $P(V)$ is located by the circuit when the switch is connected to the sample & hold output. However, when the switch is connected to $-V_{CC}$, a new value enters the sample & hold every sample time and the output of the sample & hold is the complete $P(V)$ curve for the line of video. The second position of the switch can be used when analyzing variance in $P(V)$ on a line by line basis.

The concept of computing the coordinate of the mode of $P(V)$ functions quite well in most FLIR scenes. However, should $P(V)$ be multi-peaked, noise could vary the correction level by the entire dynamic range of the system. In this case, large correction voltage could be generated due to a slight amount of noise.

3. Cumulative Distribution Technique

A second concept was investigated which eliminates the above problem. The $P(V)$ curve was integrated, therefore; the cumulative distribution resulted. This produced a smoothing effect and was, therefore; much less susceptible to noise. By definition, V_{MEDIAN} is the point where the cumulative probability distribution is 50% of maximum. For small skewness, $MEAN - MODE \approx 3 (MEAN - MEDIAN)$. Therefore, if proper scaling factors are maintained, the median contains the same information as the mode of $P(V)$. Figure 6 is a circuit block diagram which computes the mean and the median of $P(V)$ through the use of cumulative distribution rather than the density function. The circuit functions as follows: The video is integrated over each line to obtain its mean value. At the end of the line, a sample & hold maintains the mean value. The video is compared on the next line VS the mean. When the video is above the mean, the comparator output is high. The second integrator generates the cumulative probability distribution and during the horizontal blanking intervals this is subtracted from the 50% reference value. Another difference amplifier subtracts the median from the mean. The

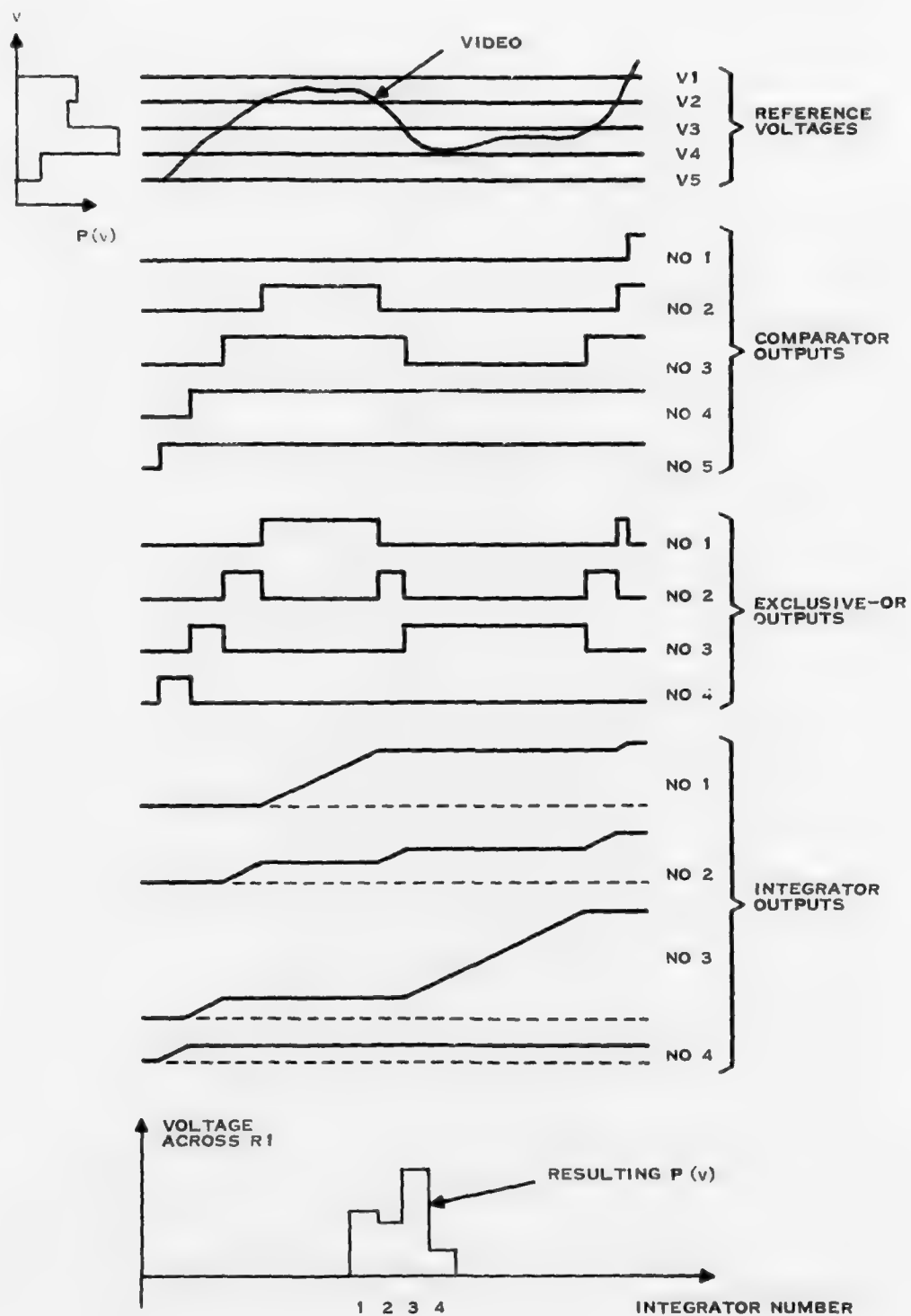


Figure 5. Typical Waveforms Dynamic Range Enhancement Scheme 1

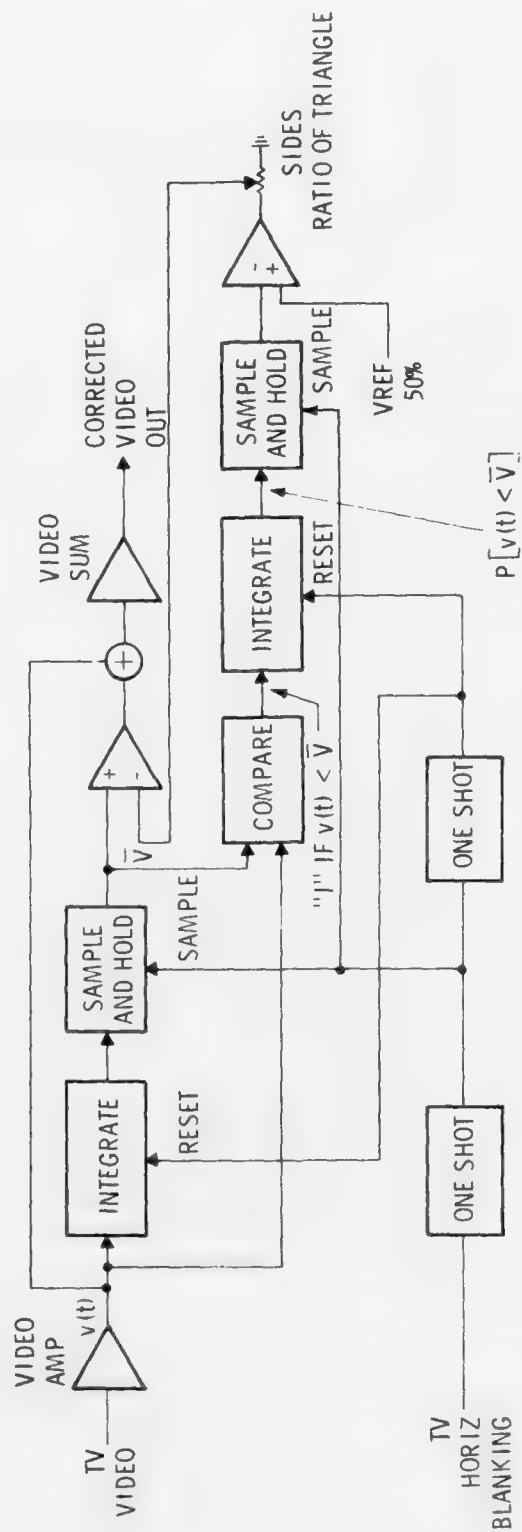


Figure 6. Dynamic Range Enhancement Scheme 2, Block Diagram

amplifier gain is adjusted to compensate for the factor of 3 and the resultant D.C. level is added to the video. The variable resistor at the output of the first difference amplifier is necessary because of axis translation needed to find the coordinate of the median of $P(V)$ (See Figure 7). Therefore, the coordinate of the median is subtracted from the coordinate of the mean. The resulting voltage is the necessary correction voltage.

Both DRE concepts contain a fallacy in the correction voltage sign for streaking targets which are larger than half the field of view in the horizontal direction. Referring to the cumulative distribution circuit of Figure 6, the problem occurs in the subtraction of $P[V(t) < \bar{V}]$ and the 50% reference level which is equal to V median. It is this difference amplifier which generates the value called ΔP in Figure 7. The variable resistor shown on the output of the difference amplifier adjusts the proportionality constant, K , so that $\Delta V = K\Delta P$. If the probability density skew becomes large, K can no longer be considered a constant and this results in a source of error.

An additional source of error results from a dependence on extended targets. For small targets (less than half the FOV) the quantity $P[V(t) < \bar{V}]$ is always greater than V median. For this case the output of the difference amplifier (ΔP) is always negative. This results in a positive correction voltage being added to the video. If the streaking target becomes greater than half the field of view, $P[V(t) < \bar{V}] < V$ median the ΔP becomes positive and a negative correction is added to the video. This, of course, enhances the streak rather than reducing it. To avoid the preceeding pitfall it would be necessary to incorporate a pattern recognition circuit to determine the spatial size of a streaking target.

The cumulative distribution technique was considered more reliable than the direct $P(V)$ method in the presence of noise. A breadboard of this method was constructed and evaluated in the laboratory using standard television video as an input. A test target was constructed which simulated streaking video while maintaining a constant value for the mean of the field. Therefore, the test target simulates AC coupled FLIR video where the mean value is zero. The target was illuminated and the camera video was processed by the DRE breadboard. The processed video was examined for proper correction and for noise which may have been added during processing. As predicted, it was observed from this test that the DRE circuit has difficulty correcting spacially large targets in the field of view. For example, a FLIR scene, which is a tilted horizon. It is desirable to display detail on the monitor of both the earth and the sky on all TV lines. With the cumulative distribution enhancement technique alone, either the earth or the sky could be in saturation depending on FLIR gain and level settings.

To help remedy the difficulties in this type of scene, a comb filter was added prior to the cumulative distribution calculation circuits. The purpose of the comb filter is to remove the fundamental horizontal frequency and its first five harmonics. The notches of the comb filter are sufficiently narrow to prevent other video from getting lost. This technique maintains midband and high frequency video response but reduces high amplitude, low frequency fluctuations. In affect, the comb filter brings the two distinct levels of video on a

TV line closer together in intensity. The output of the comb filter is then fed to the cumulative distribution circuits. All analysis of the cumulative distribution technique is based on the assumption of slightly skewed probability density. The comb filter insures that small skew is maintained.

Comb Filter

The concept of a comb filter came about from a need to put the available video information into the range of the FLIR dynamic range. The basis of operation is to place "notches" in the frequency domain. The notches are placed at the horizontal rate and multiples of it (f_H , $2f_H$, $3f_H$, . . .) and will attenuate video signals that occur at multiples of the horizontal rate (step signals such as a tilted horizon scene).

The notches must be adjustable for variable depth to prevent the resultant display from being washed out to the eye (i.e., contains false contrast information). By adjusting the depth, the signal attenuation is varied such that this washed out effect does not appear (although false contrast information still exists).

Traditionally, video filters cause display distortion because of non-linear phase response and ringing. These problems will be discussed below.

COORDINATE TRANSLATION

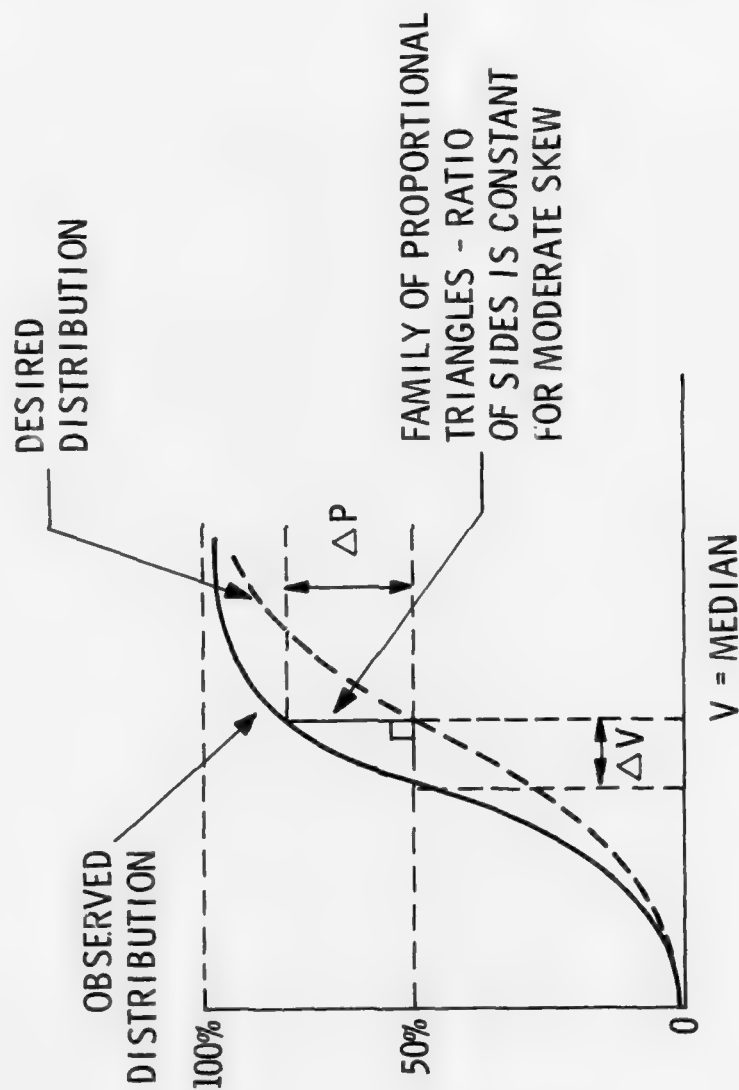
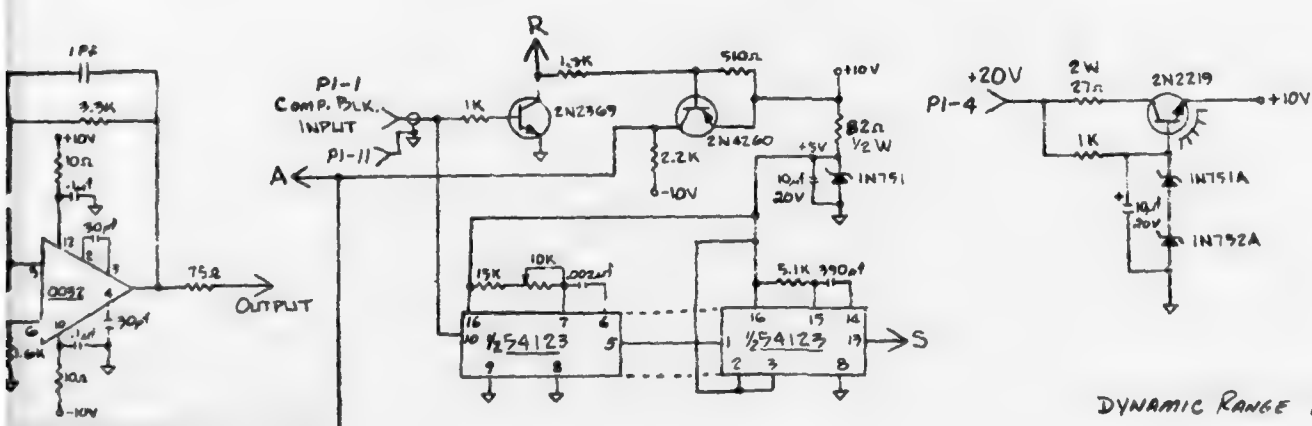
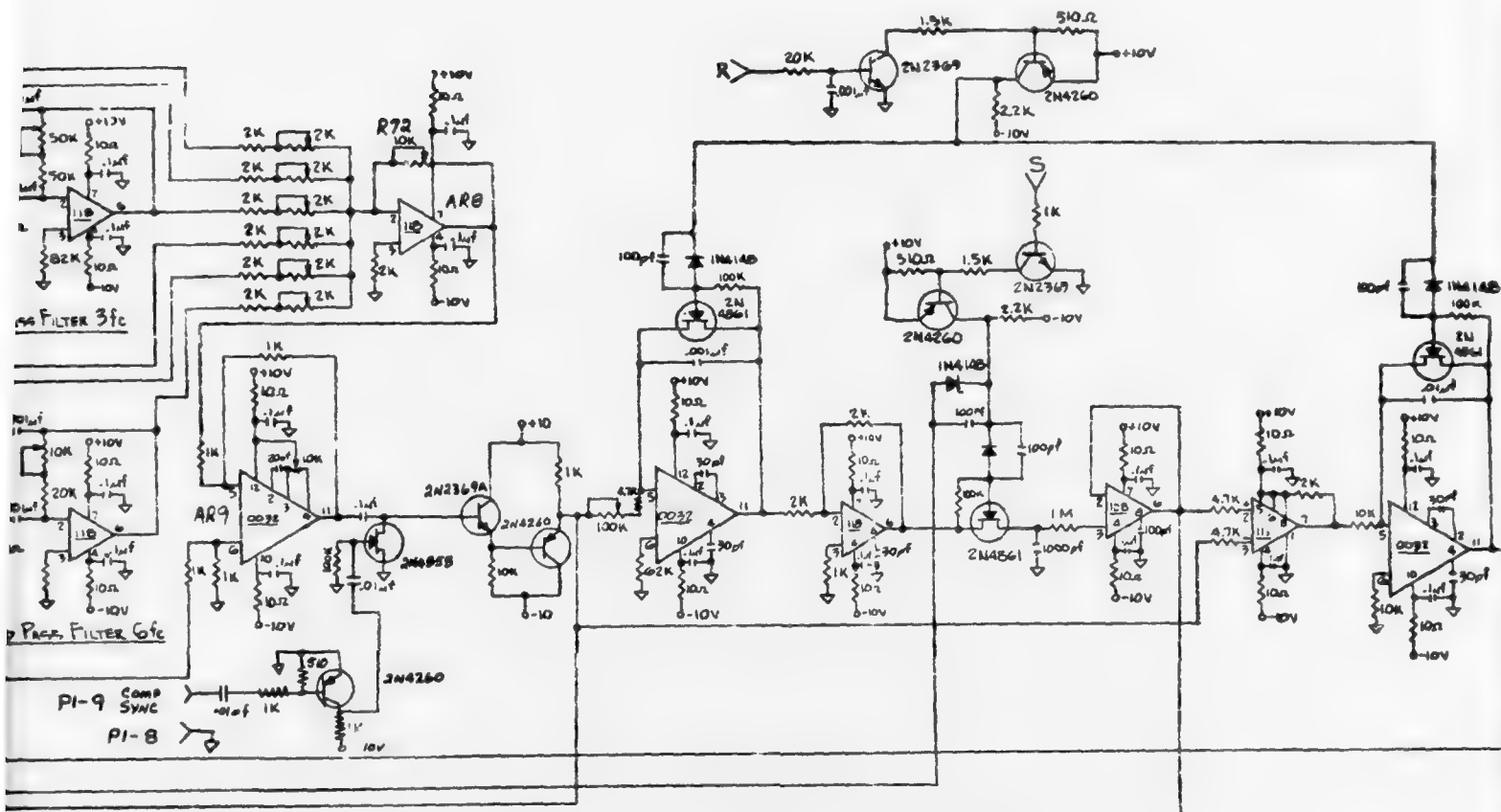


Figure 7. Coordinate Translation



DYNAMIC RANGE EXPANSION

D.E.S. 315246

PWB 315247

ASSY 315248

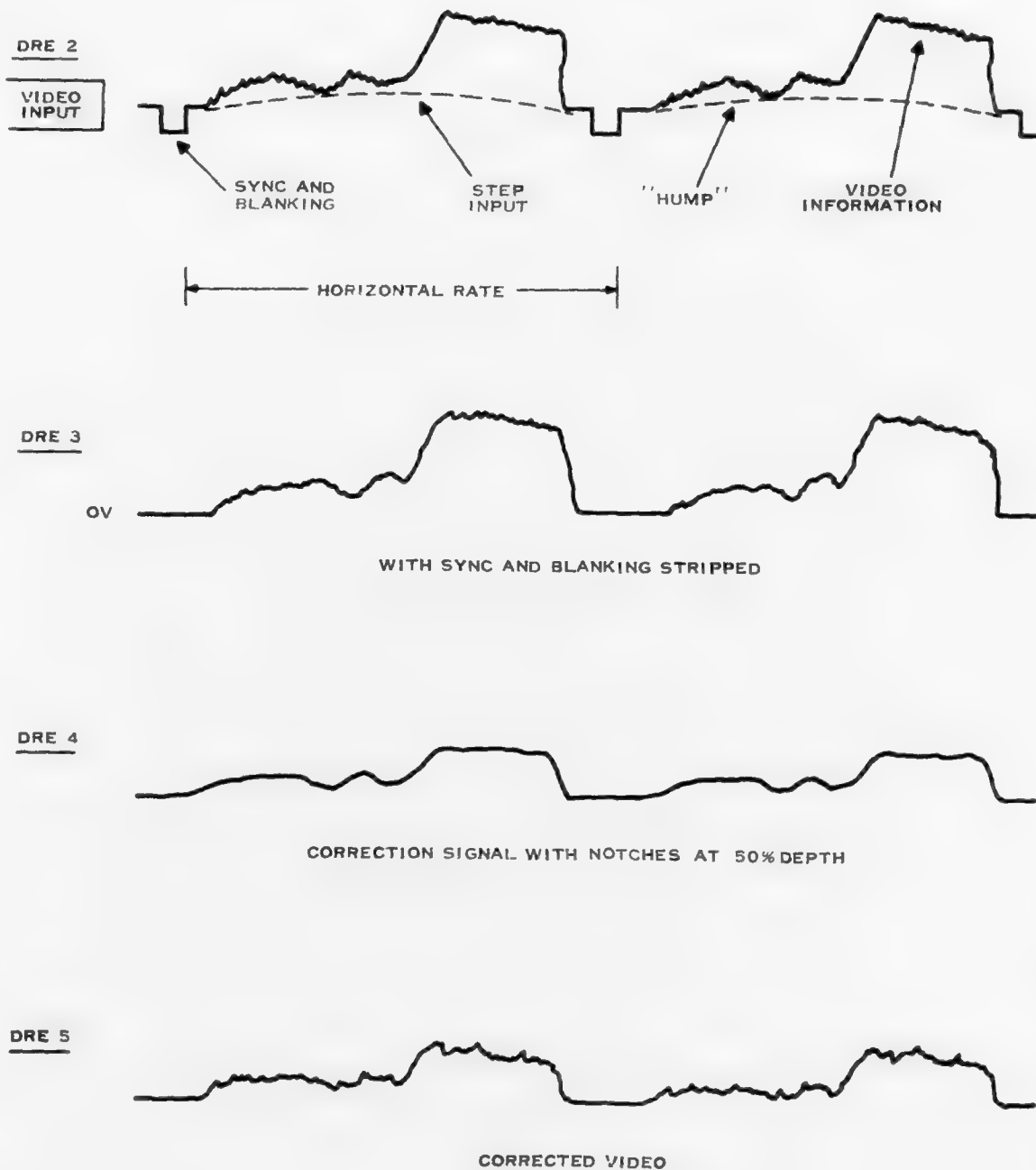


Figure 9. DRE 2,3,4,5

Circuit design explanation will be discussed below with reference to dynamic range expansion schematic (Figure 8). Incoming video, as shown in DRE2 (Figure 9) contains horizontal sync and blanking, a step input (tilting horizon scene) with video information on both levels, and a small amount of "hump" (usually from the FLIR shroud). Transistor Q1 is used to remove video sync and blanking (DRE 3 Figure 9). An ideal comb filter would contain infinite notches. This would eliminate any ringing in a step response by attenuating all Fourier components of a step input. For the DRE scheme it was evident that six notches produce an acceptable display (although more are desirable). The notches are produced by subtracting signals from the bandpass filters (f_c , $2f_c$, $3f_c$, $4f_c$, $5f_c$, $6f_c$) from the video bandpass in amplifier AR9. The problem of phase is addressed by designing high Q bandpass filters for the six filters above. These bandpass filters have a 180° phase shift at their center frequency. This signal is then inverted in AR8 to give 360° phase shift, or the signal is in phase which allows it to be subtracted from the video in AR9. By using high Q filters, signal levels are decreased appreciably when signal frequency is away from the center frequencies of the filter. This means that phase shift in the passbands is practically nil.

The resultant sum of the bandpass filters, or the correction signal (DRE 4 Figure 9), to be subtracted from the video is adjusted in amplitude by R72 in amplifier AR8. This has the effect of varying the depth of the notches. The resultant video signal out of AR9 (DRE 5 Figure 9) should be noted for several things:

- 1) The step input has been reduced bringing available video into the FLIR dynamic range.
- 2) FLIR "hump" has been reduced.
- 3) Higher frequency scene information has been reproduced without distortion.

NOTE: In the actual DRE board ringing can be noticed at the edges of a sharp step response because only six notches have been used.

With the comb filter incorporated in the DRE breadboard, the circuits were interfaced with a FLIR for roof top test. Preliminary tests indicated satisfactory operation providing FLIR gain was kept sufficiently low so that video does not saturate in the IR front end or in the LED array. This may indicate that the DRE should be tied into the Automatic Contrast Enhancement circuitry.

5. Test Results

The following test plan was used to examine the accuracy of correction and all test results are included.

Equipment Required

Hewlett-Packard 209A or equivalent marker generator
Tektronix 453 or equivalent oscilloscope
Tektronix C-30 Scope Camera
Hewlett-Packard 8601A or equivalent sweep generator
COHU Camera Test Light Box
Constant Mean Test Target
Conrac Monitor
Retma Resolution Chart

1 Laboratory Tests

1.1 Using the Hewlett-Packard 8601 as an input to the DRE, adjust the input amplitude for 0.5 VAC.

1.2 Adjust the following controls as indicated:

CONTROL	POSITION
Sweep Range	11 MHz
Sweep Mode	Video

1.3 Adjust R72 for a DRE comb filter amplitude of 0.

1.4 Connect the Tektronic 453 Scope to the output of the DRE and verify that the comb filter is not affecting the bandpass of the Video Amplifier.

1.5 Photograph the bandpass with the Sweep Marker set to 8.5 MHz. The bandpass shall be flat within ± 1 dB from 30 Hz to 8.5 MHz (Data Photo No. 1 Figure 10).

1.6 Adjust R72 until the comb filter notches appear in the passband. Verify that the six notches occur at the fundamental horizontal rate (26.25 KHz) and the first five harmonics. This can be done by using the Marker Generator and reading the frequency of the marker generator dial.

1.7 Remove the Sweep Generator and insert the camera head video as input to the DRE.

1.8 Station the camera to view the constant mean test target using back illumination provided by the light box.

1.9 Photograph DRE input (Data Photo #2 Figure 10) and output (Data Photo #3 Figure 10) video with the Oscilloscope HORIZONTAL set at 2 milliseconds per division.

- 1.10 Repeat the photographs with the Oscilloscope horizontal set at 10 μ seconds per division and a corrected video line selected. (Data Photo #4 & #5 Figure 10).
- 1.11 Exchange the constant mean target with the RETMA resolution chart. The scope shall display a single TV line containing a high resolution target.
- 1.12 Photograph the line of video with the DRE disabled (Data Photo #6 Figure 10) and photograph the same line with the DRE enabled (Data Photo #7 Figure 10).
- 2 Roof Top Tests
 - 2.1 Install the DRE in a compatible FLIR system and view outdoor scenes.
 - 2.2 Adjust the FLIR Gain and Level controls to eliminate video from being saturated in the IR amplifiers.
 - 2.3 Locate targets causing level shifts in the displayed image and video tape three or more temperature/size product targets with the DRE ON and OFF.
 - 2.4 Repeat paragraph 2.3 test with the IR Gain adjusted to cause some saturation in the IR amplifiers and video tape.
 - 2.5 Repeat paragraph 2.3 test with the IR Gain adjusted to a low level to attain a very low contrast 2.6. Switch the DRE ON and OFF and video tape any image artifact or noise which may be caused by the DRE.

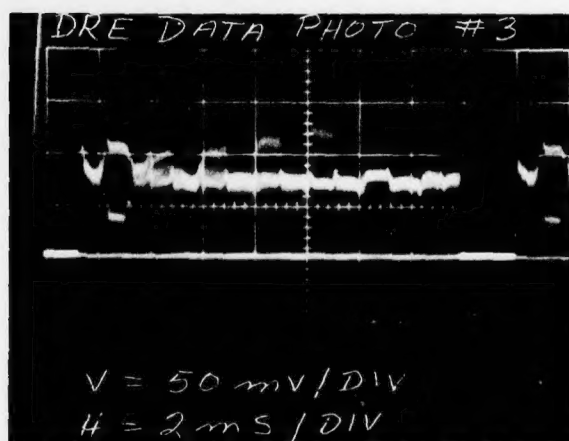
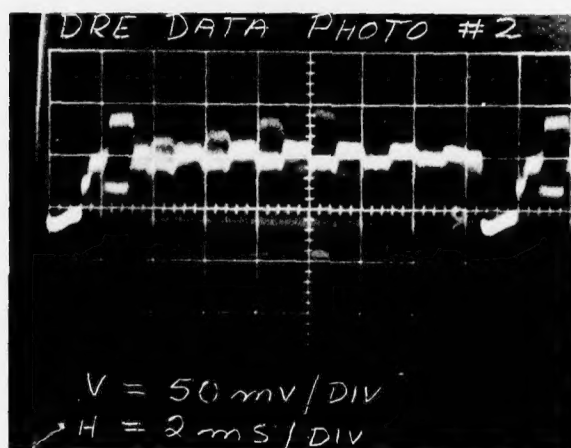
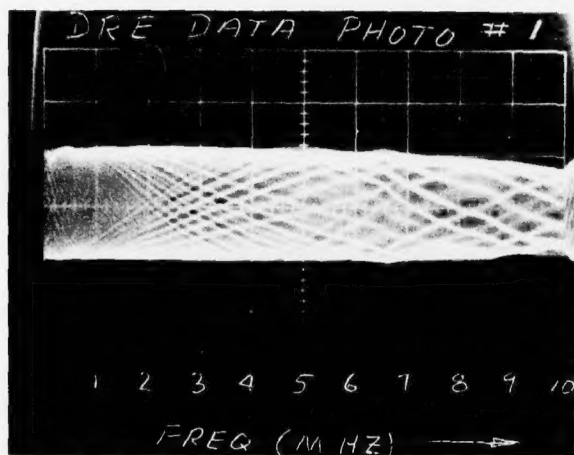


Figure 10. DRE Data Photos
 22

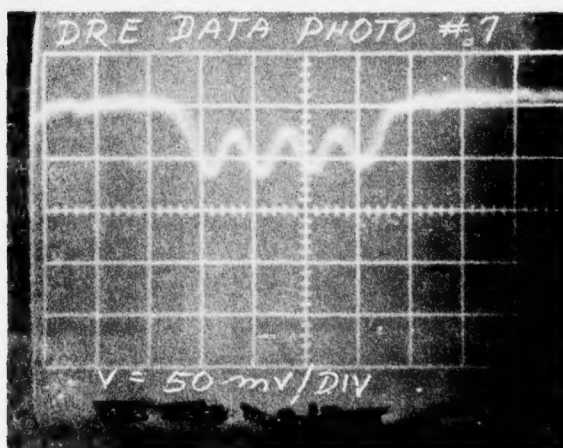
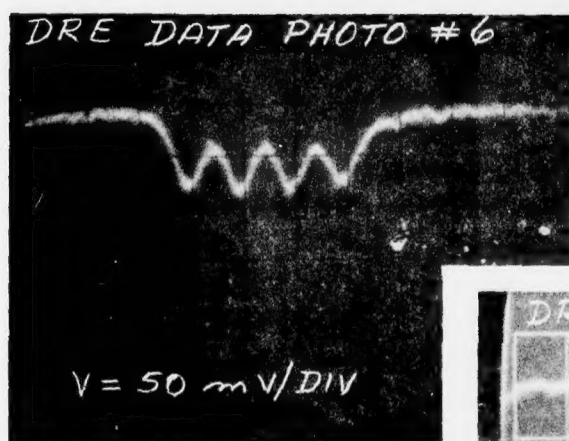
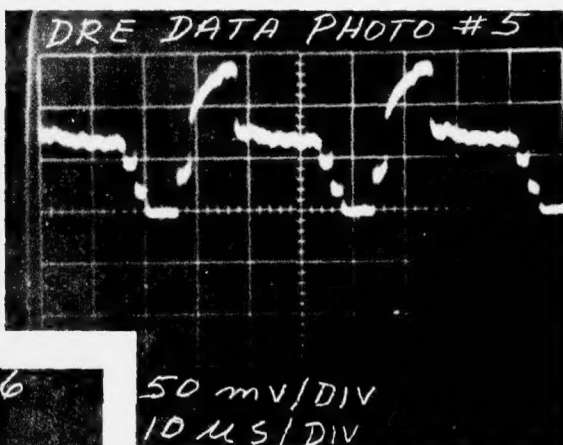
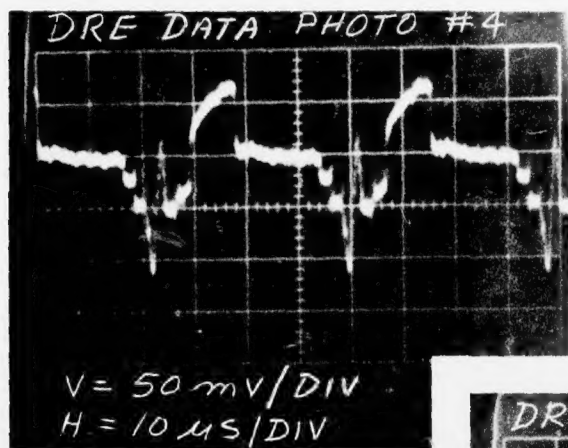


Figure 10. DRE Data Photos (Cont'd)